Coherent Quantum Optics Phenomena in Carbon Low-Dimensional Systems

Alla Dovlatova (a), Dmitri Yerchuck (b)
(a) - M.V.Lomonosov Moscow State University, Moscow, 119899,
(b) Heat-Mass Transfer Institute of National Academy of Sciences of RB, Brovka Str.15, Minsk, 220072
(Dated: December 19, 2011)

Brief review of the theoretical and experimental results, based mainly on the works of authors, in the application of quantum field theory to the study of carbon low-dimensional systems - quasi-1D carbon nanotubes, carbynes and graphene with emphasis on formation of longlived coherent states of joint photon-electron and joint resonance phonon-electron systems of given materials is presented.

PACS numbers: 78.20.Bh, 75.10.Pq, 11.30.-j, 42.50.Ct, 76.50.+g
Keywords: quantum field theory, coherent state, quasi-1D carbon nanotubes, carbynes, graphene

I. INTRODUCTION

The use of optical and radio spectroscopy methods to create coherent states in solid materials has many potential applications, ranging from nonlinear optics to solid-state quantum computing. The interest in optical or microwave methods of coherent state formation lies in existing at present many studies in the fact, that the coherent states of point centers in crystals can be efficiently excited and manipulated using optical laser fields or almost monochromatic microwave field since there are point centers in crystals (for example, substitual phosphor donor atoms in Si and N-V centers in diamond single crystals), which are relatively weakly coupled to the surrounding host lattice atoms and hence have the long coherence lifetimes needed for instance, for various optoelectronic and spintronic devices and for elaboration of quantum computing.

It seems to be very substantial for practical applications and even necessary the development of the theory, which allows to predict the appropriate electronic systems and the conditions for the formation of coherent states with more long life time. Subsequent progress in given field seems to be connected with the elaboration of theoretical models based on quantum field theory (QFT) including quantum electrodynamics (QED). Really, quantum field theory, in fact, becomes to be working instrument in spectroscopy studies and industrial spectroscopy control. Moreover, we will show in given report, that quantized electromagnetic (EM) field itself and quantized field of lattice deformations (phonon field) will be in the nearest future the working components of optoelectronic, spintronic devices and various logic quantum systems including quantum computers and quantum communication systems.

We will also show in present work the other ways to obtain long-lived coherent states with similar or even more extensive field of practical application to be consequence of more long lifetimes. Main difference of given states, that they are collective coherent states in comparison with individual coherent states, realised on point centers, which are subject of many theoretical and experimental studies, known from literature.

The aim of the work presented is to review briefly the theoretical and experimental results, based mainly on the works of authors, in the application of QFT to elaboration of new ways of long-lived coherent states' formation and its experimental confirmation on the example of carbon low-dimensional systems - quasi-1D carbon nanotubes, carbynes and graphene.

The simplest models which capture the salient features of the relevant physics in field of practical application of QED are the Jaynes-Cummings model (JCM) [2] for the one qubit case and its generalization for multiqubit systems by Tavis and Cummings [3]. Tavis-Cummings model was generalized in [4] (SYHB-model), by taking into account the 1D-coupling between qubits. Recently QED-model for single chain coupled qubit system was generalized for quasionedimensional axially symmetric multichain coupled qubit system [5]. It is substantial, that in the model, proposed in [5] (DY-model) the interaction of quantized EM-field with multichain qubit system is considered by taking into account both the intrachain and interchain qubit coupling without restriction on their values. From theoretical results in [4], [5], [6] and from their experimental confirmation in [7] follows, that by strong interaction of EM-field with matter the correct description of spectroscopic transitions including stationary spectroscopy is achieved the only in the frame of QED consideration. It concerns both optical and radio spectroscopies, that means, that QED consideration has to be also undertaken by electron spin resonance (ESR) studies in the case of strong interaction of EM-field with spin systems. The review of given results is given in Section 2.

It is reasonable to suggest, that analogous conclusion can be drawn for the case of strong interaction of phonons with spin system or electron system. In other words it seems to be reasonable the idea, that relaxation of paramagnetic (or optical) centers in the case of strong spin-phonon (electron-phonon) interaction can be described correctly the only in the frames of quantum field theory. The system of equations for dynamics of spectroscopic transitions in 1D multiqubit exchange coupled (para)magnetic and optical systems by strong dipole-photon and dipole-phonon coupling within the framework of quantum electrodynamics and quantum defor-

mation field theory phonon theory was derived in [8]. It was showed, that new quantum physics phenomenon - the formation of longlived coherent state of joint systems {electric(magnetic) dipoles + resonance phonons}, leading to appearance of quantum acoustic (phonon) Rabi oscillations has to be taking place. The results obtained are reviewed in Section 3.

Let us also remark, that in all theoretical and experimental studies of the matter systems by means of stationary optical- and radio spectroscopy methods EM-field is considered the only classically. For example, in relatively recent work [1] the review of development in the theory of resonant Raman scattering (RS) in 1D electron systems is given by using several different quantum theoretical models of the matter subsystem - Fermi liquid model, Luttinger liquid model and Hubbard model, however by classical description of EM-field.

II. LONGLIVED COHERENT STATE FORMATION IN CARBON LOW-DIMENSIONAL MATERIALS IN RESULT OF RABI-WAVE PACKETS' PROPAGATION

QED-model for multichain coupled qubit system, that is DY-model, proposed in [5] predicts, that by strong electron-photon interaction quantum nature of EM-field can become apparent in any stationary optical experiments. In particular, new quantum optics phenomenon - Rabi waves and Rabi wave packets' formation, which was theoretically predicted for the fist time in [4], can give essential contribution in stationary spectral distribution of Raman scattering (RS) intensity and spectral distributions of infrared (IR), visible or ultraviolet absorption, reflection, transmission intensities. The calculation [5] is illustrated on the example of perfect quasi-one-dimensional carbon zigzag shaped carbon nanotubes (CZSNTs). In fact 2D-1D transition appearance (new quantum size effect) in physical properties of carbon nanotubes, which is realised with diameter decrease, is theoretically argued. It is predicted, that 2D-1D transition leads to necessity of qualitatively different electronic model for quasi-1D CZSNTs with cardinal change of their physical properties. The electronic model for quasi-1D CZSNIt is the following. The single quasi-1D CZSNT represents itself autonomous dynamical system with discrete circular symmetry, consisting of finite number $n \in N$ of carbon backbones of trans-polyacetylene (t-PA) chains, which are placed periodically along transverse angle coordinate. Longitudinal axes $\{x_i\}$, $i = \overline{(1,n)}$, of individual chains can be directed both along element of cylinder and along generatrix of any other smooth figure with axial symmetry. It is similar to Su, Schrieffer, Heeger (SSH) [9], [10] model of 1D organic conductors in the part, concerning the choose of active degrees of freedom, that allows to consider all n carbon chains in the model of quasi-1D CZSNTs to be equivalent each other, while in real quasi-1D CZSNTs the adjacent chains represent themselves a mirror of each other relatively corresponding planes, passing through NT-axis. Given n-chain set can be considered to be a single whole, which holds the quasi-one-dimensionality of a single chain. It seems to be correct for perfect CZSNTs, if their diameter is ≤ 1 nm .

At the same time it is well known, that free standing nanotubes are considered theoretically to be $2D$-strutures and two-dimensional lattice structure of a single wall carbon nanotube (SWNT) is determined by the chirality, which is defined by two integers (n, m) [11], [12]. Two in-plane G point longitudinal and transverse optical phonon (LO and TO) modes [13] and the out-of-plane radial breathing mode (RBM) [14] are observed in the Raman spectra of SWNTs. The LO and TO phonon modes at the G point in the two-dimensional Brillouin zone are degenerate in 3D-graphite and 2D-graphene, however they split in SWNTs into two peaks, denoted by G^+ and G^-peaks, respectively, [15]. It is consequence of the curvature effect. The agreement of experimental Raman studies of carbon nanotubes (NTs) with diameter $\geq 1nm$ with $2D$ SWNT-theory unambiguously indicates, that given NTs, produced mainly by various CVD-methods are really $2D$ systems (in cylindric space). At the same time the narrow NTs with diameter $< 1nm$ cannot be considered strongly speaking to be $2D$-systems, they are quasi-$1D$ systems, and in [5] and in [7] is argued, that 2D-1D transition (quantum size effect) has to be take place and it really takes place by its control with radiospectroscopy methods.

At the same time the presence of both intrachain and interchain qubit coupling by simultaneous preservation of quasionedimensionality seems to be leading to additional requirements for observation of size effects by 2D-1D transition, especially with optical methods, which are very sensitive to structural perfectness. It is understandable, that along with requirement of quasionedimensionality the additional requirement of homogeneity of the ensemble of NTs arises. It means, that any dispersion in axis direction, chirality, length and especially in diameter both for single NT along its axis and between different NTs in ensemble has to be absent, axial symmetry has to be also retained, that is, there are additional requirements in comparison with, for example, t-PA technology. The CVD-technology of NTs production and many similar to its seem to be not satisfying to above-listed requirements at present. It means, that experimental results and their theoretical treatment will be different in both the cases, that really takes place. The situation seems to be analogous to some extent to the solid state physics of the same substance in single crystal- and amorphous forms. It was shown in [7], that the technology of CZSNTs formation, based on high energy ion beam modification (HEIBM) of natural diamond single crystals, satisfy given requirements.

Semiclassical evaluation, obtained in [5], has led to conclusion, that π-subsystem of quasi-1D CZSNTs will be inactive in optical experiments. The comparison with

optical properties of related carbon chain material - carbynoids - has allowed to predict, that among possible optically active topological defects in σ-subsystem of quasi-1D CZSNTs the σ-polaron is expected to be prevailing.

Each σ-polaron interacting with external EM-field in accordance with experiment in [26] can be approximated like to guantum dots in [4] by two-level qubit. Then the Hamiltonian, proposed in the work [4] can be generalized, that was done. The insufficient for the model local field term was omitted. (Local field term seems to be playing minor role by description of σ-polarons in comparison with quantum dots, since size of quantum dots is greatly exceeding the size of σ-polarons). The apparatus of hypercomplex n-numbers was used. Hypercomplex n-numbers are defined to be elements of commutative ring, given by (1)

$$Z_n = C \oplus C \oplus ... \oplus C, \tag{1}$$

$Z_1 = C$. that is, it is direct sum of n fields of complex numbers C, $n \in N$. It means, that any hypercomplex n-number z is n-dimensional quantity with the components $k_\alpha \in C$, $\alpha = \overline{0, n-1}$, that is in row matrix form z is

$$z = [k_0, k_1, k_2, ..., k_{n-1}]. \tag{2}$$

Hypercomplex n-number z can be represented also in the form

$$z = \sum_{\alpha=0}^{n-1} k_\alpha \pi_\alpha, \tag{3}$$

where π_α are basis elements of Z_n. They are

$$\begin{array}{l} \pi_0 = [1, 0, ..., 0, 0], \pi_1 = [0, 1, ..., 0, 0], \\ ..., \pi_{n-1} = [0, 0, ..., 0, 1]. \end{array} \tag{4}$$

In other words, the set of $k_\alpha \in C, \alpha = \overline{0, n-1}$ is the set of eigenvalues of hypercomplex n-number $z \in Z_n$, the set of $\{\pi_\alpha\}$, $\alpha = \overline{0, n-1}$ is eigenbasis of Z_n-algebra. Then the QED-Hamiltonian, considered to be hypercomplex operator n-number, for σ-polaron system of interacting with EM-field CZSNTs, consisting of n backbones of t-PA chains, which are connected between themselves in that way, in order to produce rolled up graphene sheet, in matrix representation is

$$[\hat{\mathcal{H}}] = [\hat{\mathcal{H}}_\sigma] + [\hat{\mathcal{H}}_F] + [\hat{\mathcal{H}}_{\sigma F}] + [\hat{\mathcal{H}}_{\sigma\sigma}]. \tag{5}$$

The rotating wave approximation and the single-mode approximation of EM-field are used. All the components in (5) are considered to be hypercomplex operator n-numbers and they are the following. $[\hat{\mathcal{H}}_\sigma]$ represents the operator of the energy of σ-polaron subsystem in the absence of interaction between σ-polarons themselves and with EM-field. It is

$$[\hat{\mathcal{H}}_\sigma] = (\hbar\omega_0/2) \sum_{j=0}^{n-1} \sum_m \hat{\sigma}^z_{mj} [e_1]^j, \tag{6}$$

where $\hat{\sigma}^z_{mj} = |a_{mj}\rangle \langle a_{mj}| - |b_{mj}\rangle \langle b_{mj}|$ is z-transition operator between the ground and excited states of m-th σ-polaron in j-th chain. The second term

$$[\hat{\mathcal{H}}_F] = \hbar\omega \sum_{j=0}^{n-1} \hat{a}^+ \hat{a} [e_1]^j \tag{7}$$

is the Hamiltonian of the free EM-field, represented in the form of hypercomplex operator n-number. The component of the Hamiltonian (5)

$$[\hat{\mathcal{H}}_{\sigma F}] = \hbar g \sum_{j=0}^{n-1} \sum_m (\hat{\sigma}^+_{mj} \hat{a} e^{ikma} + \hat{\sigma}^-_{mj} \hat{a}^+ e^{-ikma}) [e_1]^j \tag{8}$$

corresponds to the interaction of σ-polaron sybsystem with EM-field, where g is the interaction constant. The next term in Hamiltonian (5) describes the intrachain and interchain σ-polaron–σ-polaron interaction. It is given by the expression

$$\begin{array}{l} [\hat{\mathcal{H}}_{\sigma\sigma}] = -\hbar \sum_{l=0}^{n-1} \sum_{j=0}^{n-1} \xi^{(1)}_{|l-j|} [e_1]^l \sum_m |a_{mj}\rangle \langle a_{m+1,j}| [e_1]^j \\ - \hbar \sum_{l=0}^{n-1} \sum_{j=0}^{n-1} \xi^{(1)}_{|l-j|} [e_1]^l \sum_m |a_{mj}\rangle \langle a_{m-1,j}| [e_1]^j \\ - \hbar \sum_{l=0}^{n-1} \sum_{j=0}^{n-1} \xi^{(2)}_{|l-j|} [e_1]^l \sum_m |b_{mj}\rangle \langle b_{m+1,j}| [e_1]^j \\ - \hbar \sum_{l=0}^{n-1} \sum_{j=0}^{n-1} \xi^{(2)}_{|l-j|} [e_1]^l \sum_m |b_{mj}\rangle \langle b_{p-1,j}| [e_1]^j, \end{array} \tag{9}$$

where $\hbar\xi^{(1,2)}_{|l-j|}$ are the energies, characterising intrachain ($l = j$) and interchain ($l \neq j$) σ-polaron–σ-polaron interaction for the excited ($\xi^{(1)}$) and ground ($\xi^{(2)}$) states of j-th chain, $|b_{mj}\rangle, |a_{mj}\rangle$ are ground and excited states correspondingly of m-th σ-polaron of j-th chain. Matrix $[e_1]^j$ in (6) to (9) is j-th power of the circulant matrix $[e_1]$, which is the following

$$[e_1] = \begin{bmatrix} 0 & 1 & 0 & ... & 0 \\ 0 & 0 & 1 & ... & 0 \\ & ... & & & \\ 0 & 0 & ... & 0 & 1 \\ 1 & 0 & ... & 0 & 0 \end{bmatrix}. \tag{10}$$

The solution of nonstationary Schrödinger equation for hypercomplex matrix function, determined by

$$\begin{array}{l} [|\Psi(t)\rangle] = \\ \sum_{j=0}^{n-1} \{ \sum_l \sum_m \left(A^j_{m,l}(t) |a_{mj}, l\rangle + B^j_{m,l}(t) |b_{mj}, l\rangle \right) \} [e_1]^j. \end{array} \tag{11}$$

where $|b_{mj}, l\rangle = |b_{mj}\rangle \otimes |l\rangle$, $|a_{mj}, l\rangle = |a_{mj}\rangle \otimes |l\rangle$, $|l\rangle$ is the EM-field Fock state with l photons, $A^j_{m,l}(t)$, $B^j_{m,l}(t)$

are the unknown probability amplitudes, was obtained in continuum limit ($[|\Psi(t)_{cont}\rangle] \equiv [|\Phi^l(x,t)\rangle]$) and it was represented in the form of sum of n solutions for n chains, that is, hypercomplex n-number $\Phi^l(x,t)$ is

$$\Phi^l(x,t) = \sum_{q=0}^{n-1} \tilde{\Phi}^l_q(x,t), \tag{12}$$

where the solution for q-th chain $\tilde{\Phi}^l_q(x,t)$ is

$$\tilde{\Phi}^l_q(x,t) = \sum_{p=0}^{n-1} \Phi^l_{qp}(x,t)[e_1]^p, \tag{13}$$

in which the matrix elements $\Phi^l_{qp}(x,t)$ of matrix $[\Phi^l(x,t)]$ are

$$\Phi^l_{qp}(x,t) = \int_{-\infty}^{\infty} \Theta^l_q(h,0) \exp\frac{-2\pi qpi}{n} \exp ihx \times \\ \exp\{i\sum_{j=0}^{n-1} \exp\frac{2\pi qji}{n}(\vartheta_j(h) - g\sqrt{l-1}\kappa_j(h))\}dh, \tag{14}$$

where $\Theta^l_q(h,0)$, $\vartheta_j(h)$, $\kappa_j(h)$ are determined by eigenvalues $\mathbf{k}_\alpha \in C, \alpha = \overline{0,n-1}$ of $\Phi^l(h,0)$, $\theta(h)$ and $\chi(h)$, which are considered to be hypercomplex n-numbers. They are

$$\Theta^l_q(h,0) = \frac{1}{n}\mathbf{k}_q(\Phi^l(h,0)) = \frac{1}{n}\sum_{j=0}^{n-1} \Phi^l_j(h,0) \exp\frac{2\pi qji}{n} \tag{15}$$

$$\vartheta_j(h) = \frac{1}{n}\mathbf{k}_j(\theta(h)) = \frac{1}{n}\sum_{r=0}^{n-1} \theta_r(h) \exp\frac{2\pi jri}{n}, \tag{16}$$

$$\kappa_j(h) = \frac{1}{n}\mathbf{k}_j(\chi(h)) = \frac{1}{n}\sum_{r=0}^{n-1} \chi_j(h) \exp\frac{2\pi jri}{n}. \tag{17}$$

It was taken into account, that for the state vector $[|\Psi(t)\rangle]_c ont$ in continuum limit we have

$$[\Phi^l(x,t)] = \\ \int_{-\infty}^{\infty} [\overline{\Phi}^l(h,0)] \exp\{it([\theta^l(h)] - g\sqrt{l+1}[\chi])\}e^{ihx}dh, \tag{18}$$

where x is hypercomplex axis $x = [x,x,...,x]$, $[\Phi^l(x,t)]$ is

$$[\Phi^l(x,t)] = exp\frac{i(\omega_0 t - kx)[\sigma_z]}{2} \exp\frac{\lambda t}{2}[\Psi^l(x,t)], \tag{19}$$

In its turn $[\Psi^l(x,t)]$ is continuous limit of functional block matrix of discrete variable m, which is given by (20).

$$[\Psi_{m,l}(t)] = \begin{bmatrix} [A_{m,l}(t)] \\ \\ [B_{m,l+1}(t)] \end{bmatrix}, \tag{20}$$

consisting of two $[n \times n]$ matrices of probability amplitudes

$$[A_{m,l}(t)] = \sum_{j=0}^{n-1} A^j_{m,l}(t)[e_1]^j, \\ [B_{m,l+1}(t)] = \sum_{j=0}^{n-1} B^j_{m,l+1}(t)[e_1]^j, \tag{21}$$

which are determined by relationship (11). Further, matrix $[\theta(h)]$ in (18) is

$$[\theta(h)] = \frac{1}{2}\{([\theta_1(h)] + [\theta_2(h)]) \otimes [E_2]\} \\ + \frac{1}{2}\{([\theta_1(h)] - [\theta_2(h)]) \otimes [\sigma_z]\}, \tag{22}$$

where $[\theta_1(h)]$ and $[\theta_2(h)]$ are

$$[\theta_1(h)] = [\xi_1]\{2 - a^2(h + \frac{k}{2})^2\}, \\ [\theta_2(h)] = [\xi_2]\{2 - a^2(h - \frac{k}{2})^2\} \tag{23}$$

Matrix $[\chi]$ in (18) is

$$[\chi] = [E_n] \otimes [\sigma_x] \exp(-i[\sigma_z](\omega - \omega_0)t), \tag{24}$$

where $[E_n]$ is $[n \times n]$ unit matrix.

The relationship (13) by taking into account (14) - (24) determines Rabi-wave packet, which propagates along individual chain of CZSNT. Subsequent analysis of Rabi-wave packet dynamics for individual chain in CZSNT will be now coinciding by rescaling of parameters with analysis of Rabi-wave packet dynamics in quantum dot chain, considered in [4]. In particular, in the same manner can be obtained temporal dependence of the integral inversion, which gives in implicit form the way for comparison of theoretical results with any stationary optical experiments in any quasi-1D system with strong electron-photon interaction. It is sufficient to make a Fourier transform of given temporal dependence. Fourier transformed temporal dependence of the integral inversion will be proportional to spectral distribution by IR-absorption, IR-transmission, IR-reflection or Raman scattering, since they are determined by population difference. It means, that dynamical quantum nonstationary properties of optical systems can become apparent by conventional stationary registration of the spectra.

Given conclusion was confirmed in [7] by the RS study of quasi-1D CZSNTs, IR study of carbynes and by analysis of RS results in graphene.

Samples of type IIa natural diamond, implanted by high energy ions of copper and boron (the energy of ions in ion beam is 63 MeV and 13.6 MeV for copper and boron ions correspondingly, ion beam dose is 5×10^{14} cm^{-2}) have been studied in given work. Both the samples represent in their geometry prismes with quilateral triangle in their bases, coinciding with (111) crystallographic plane, side of base triangle was equal to $\approx 5mm$,

depth of the samples was equal to $\approx 1mm$. Ion implantation was performed along $\langle 111 \rangle$ crystal direction, that is transversely to triangle prism base uniformly along all the surface.

Raman scattering (RS) spectra were registered in backscattering geometry. Laser excitation wave length was 488 nm, rectangular slit $350\times350(\mu m)^2$ was used, scan velocity was 100 cm^{-1} pro minute.

Infrared absorption and reflection studies have been performed on uniaxially oriented carbynoid film samples prepared by chemical dehydrohalogenation of poly(vinylidene fluoride) (PVDF), which were stored 12 Y at room temperature. Preparation details of carbynoids were described in [19]. The FTIR spectrometer "Nexus" has been used, IR spectra were registered in the range $400 - 5000$ cm^{-1} at room temperature. Two groups of uniaxially oriented carbynoid film samples were studied, designated correspondingly A and B samples. Carbynoid samples con- tained a rather high concentration of residual fluorine and technological oxygen atoms. The samples of A set (hereinafter A-samples, their designation in [19] is the sec- ond series samples) were with F/C ratio equal to 3/7, their oxygen contamination O/C was 1 to 5. A-samples were thermally treated at 120°C for 2 hours. The contamination of fluorine and oxygen atoms in the samples of B series (hereinafter B-samples, their designation in [19] is the third series samples) was intermediate between 3/10 and 3/7 for the F/C ratio and between 1 to 10 and 1 to 5 for O/C ratio (however O and F content was not determined exactly). Like to the classification proposed for doped t-PA [20], the samples studied can be attributed both to highly doped carbynes and to carbynoids, that is to materials including a wide range of carbyne-like structures. It was established, that the difference between the spectra for the samples, belonging to the same group is in limits of uncertainty of experimental measurements, and the spectra for two samples belonging to different groups was presented and analysed in [7].

It is seen from Figures 1, that Raman spectra are characterised in quasi-1D CZSNTs, produced by $\langle 111 \rangle$ HEIBM of diamond single crystals (in copper implanted sample by excitation from impanted side of the sample) by the only single vibronic mode of the lattice, formed by Su-Schrieffer-Heeger σ-polarons with peak position at 656.8±0.2 cm^{-1} and by additional lines with peak positions 1215±1 cm^{-1}, 1779.5±1 cm^{-1}, 2022.3±0.5 cm^{-1} corresponding to Fourier transform of revival part of of the time-dependence of integral inversion, detection of which in stationary RS-measurements is determined by formation and propagation of quantum Rabi wave packet, to be consequence of quantum nature of EM-field. Given RS-mode is appeared instead of longitudinal and transverse optical phonon G^+ and G^-modes and the out-of-plane radial breathing mode, which are observed in Raman spectra of 2D single wall nanotubes [15].

The identification of the lines 1215±1 cm^{-1}, 1779.5±1 cm^{-1}, 2022.3±0.5 cm^{-1} (and corresponding lines in

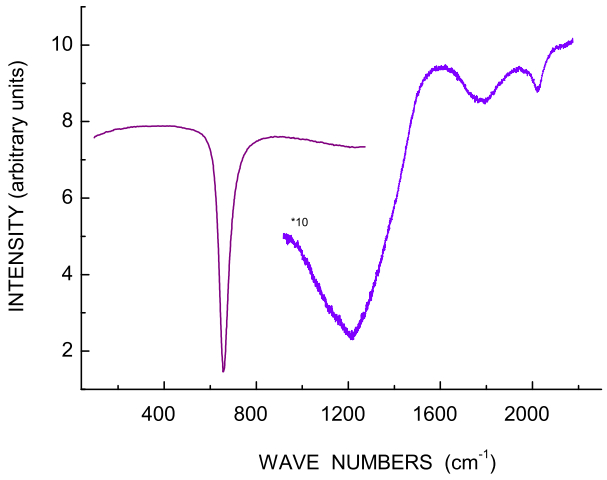

Figure 1: Spectral distribution of Raman scattering intensity in diamond single crystal, implanted by high energy copper ions, the excitation is from implanted side of the sample

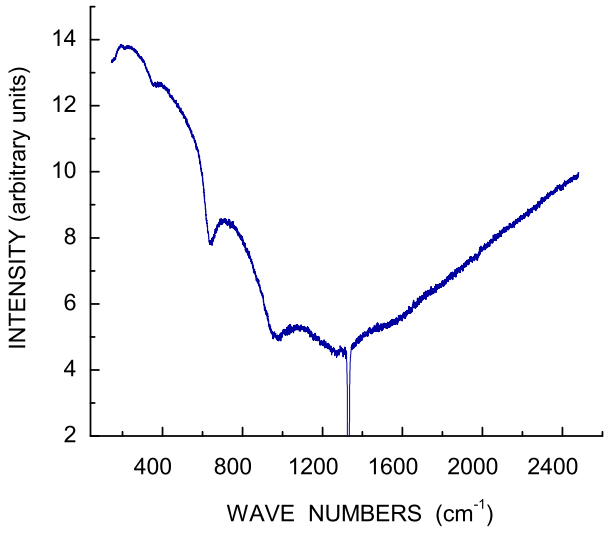

Figure 2: Spectral distribution of Raman scattering intensity in diamond single crystal, implanted by high energy copper ions, the excitation is from unimplanted side of the sample

boron ion modified sample) with Fourier-image of revival part of Rabi packet is confirmed by the following. It is well known [16], that in the case of point absorbing centers classical Rabi frequency is linear function of the amplitude of oscillating EM-field. It was experimentally confirmed in [17], [18]. Given dependency takes also place for the center of Rabi wave packet, that follows from the analysis of Fourier transform of temporal dependence of the integral inversion. Further, it is evident, that amplitude of electrical component of laser irradiation, pene-

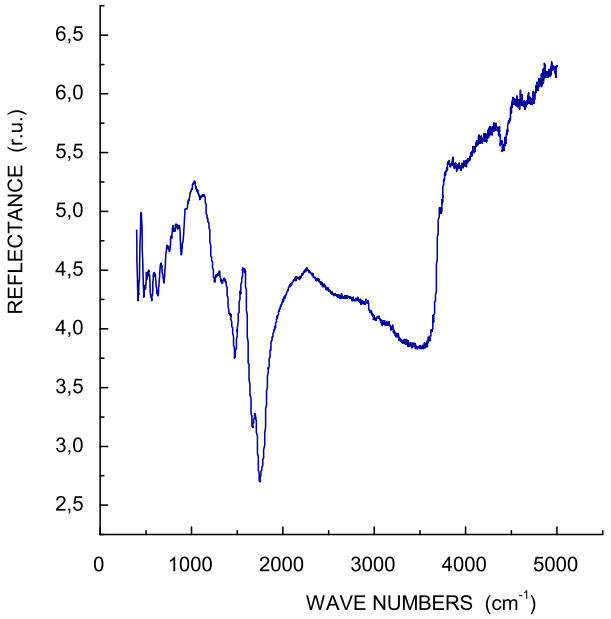

Figure 3: Spectral distribution of IR reflection intensity in carbyne uniaxially oriented A-sample

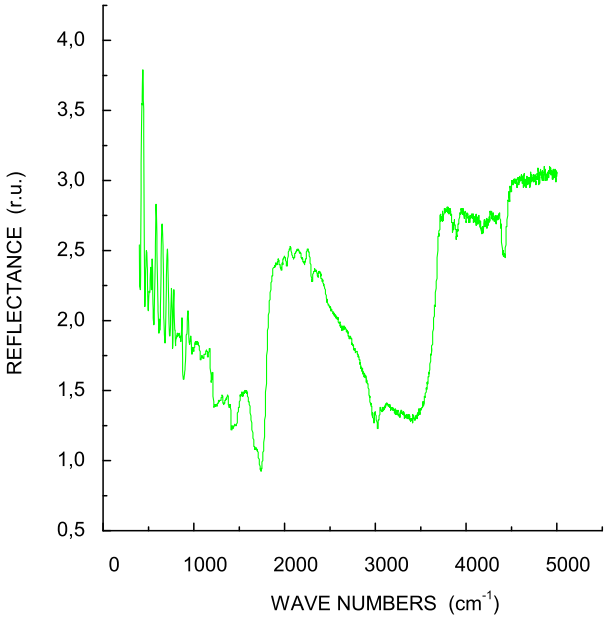

Figure 4: Spectral distribution of IR reflection intensity in carbyne uniaxially oriented B-sample

trating in ion beam modified region (IBMR), is lesser by excitation from unimplanted side. It is consequence of some absorption in the unimplanted volume of diamond crystal. We see, that really, the frequency values of additional two rightmost Raman peaks at 1569 ± 3 cm^{-1}, 1757 ± 5 cm^{-1}, which are observed in Raman spectrum by excitation of diamond sample with incorporated CZSNTs from unimplanted side are substantially less, than the frequency values of additional two rightmost spectral components at 1779.5$\pm$1 cm^{-1} and 2022.3$\pm$0.5 cm^{-1}, observed by excitation from implanted side, compare Figure 2 and Figure 1. Relative frequency changes are 1,151 and 1.134 ± 0.003 for the pairs [2022.3$\pm$0.5 cm^{-1}, 1757 ± 5 cm^{-1}] and [1779.5$\pm$1 cm^{-1}, 1569 ± 3 cm^{-1}] correspondingly and it is seen, that they are close to each other. It is substantial, that more high frequency undergoes slightly more large relative change in correspondence with theoretical analysis.

The lines at 354.6, 977.1 (± 1) cm^{-1}, Figure 2, were assigned with two antiferroelectric spin wave resonance (AFESWR) modes. It means, taking into account the conclusion on some magnetic ordering quasi-1D CZSNTs in [21] and direct observation in the same sample of ferromagnetic spin wave resonance (FMSWR) [22], [23], that quasi-1D CZSNTs are multiferroic materials. Let us remark, that AFESWR is new optical phenomenon, which was theoretically described and experinmentally confirmed for the first time in [26] by the study of optical properties of carbynes. It seems to be very interesting, that carbynes along with antiferroelectric ordering possess also by ferroelectric and ferromagnetic ordering. The

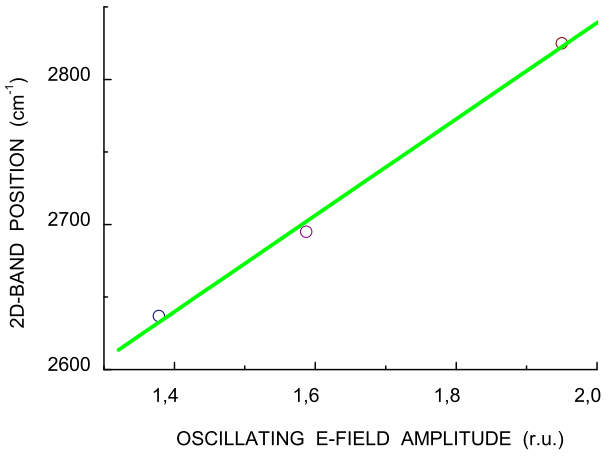

Figure 5: Dependence of $2D$-band position in graphene on electrical component of oscillating excitation field

conclusion on ferromagnetic ordering has been obtained from ESR studies of heavily doped by technological impurities carbynes in [19], [29] by means of immediate observation of ferromagnetic spin wave resonance. The optical studies of the same samples in [30], [31], [32], [27], [26], [28] allowed to estabish the origin and the structure of infrared (IR) and Raman scattering (RS) active centers, at that the conclusion on both antiferroelectric ordering and simultaneous ferroelectric ordering of carbynes was obtained directly by registration of antiferroelectric

spin wave resonance and ferroelectric spin wave resonance (FESWR) in [27], [26] and [28] respectively. Especially interesting, that both antiferroelectricity, ferroelectricity and ferromagnetism have been observed simultaneously in the same samples and, what is characteristic, in the same temperature range, in particular, at room temperature. Let us remark, that along with antiferroelectric spin wave resonance ferroelectric spin wave resonance is also new quantum physics phenomenon and it has been identified in [28] for the first time in optical spectroscopy too. Let us also remark, that given phenomenon and its characteristic features were predicted theoretically in [25].

Antiferroelectricity seems to be very new property of pure carbon at all. Moreover antiferroelectric ordering has been found in the matter for the first time (to our knowlegde).

Let us remark, that experimental observation of multiferroicity in quasi-1D CZSNTs means the breakdown of space inversion symmetry along hypercomplex CZSNT symmetry axis x. It agrees well with the model of quasi-1D CZSNTs, [5], [7], based on bond dimerisation in all chain components of quasi-1D CZSNT along its symmetry axis x, which leads to inversion symmetry breakdown along given axis. Therefore, the experimental observation of antiferroelecricity of quasi-1D CZSNTs, necessary condition of which is the evident prediction of the model, proposed in [5], can be considered to be additional argument in favour of given model.

At the same time, typical multiferroics belong to the group of the perovskite transition metal oxides, and include rare-earth manganites and -ferrites, that is, they are the compounds, which include atoms with unfilled inner d or f atomic shells (for example $TbMnO_3$, $HoMn_2O_5$, $LuFe_2O_4$). Other examples are the bismuth compounds $BiFeO_3$ and $BiMnO_3$, and non-oxides like to $BaNiF_4$ and spinel chalcogenides, for example $ZnCr_2Se_4$. These alloys show rich phase diagrams combining different ferroic orders in separate phases. Apart from single phase multiferroics, composites and heterostructures exhibiting more than one ferroic order parameter are existing. Given comparison indicated, that mechanism of multiferroicity is quite other, which is the subject of another original research.

The substantial decrease of relative intensity of 641.8 $\pm 1\ cm^{-1}$ mode in comparison with 656.8$\pm$0.2 cm^{-1} mode testifies in favour of given assignment. It is seen, that AFESWR-splitting is rather large and it has the same order of values with the splitting between two σ-polaron vibronic levels. It means, that linear AFESWR-theory [26], which predicts a set of equidistant AFESWR-modes, arranged the left and the right of central mode, can be used the only to obtain approximately the average value of AFESWR-splitting. Really, it is seen from Figure 2, that in given case AFESWR-modes are not equidistant, they are shifted on different distances 335.3, 287,2 cm^{-1} from main AFESWR-mode. At the same time average value of AFESWR-splitting is 311.3 cm^{-1} and it is close to the value in 300 cm^{-1} expected in accordance with linear AFESWR-theory by taking into account experimental AFESWR-splitting value in carbynes [26].

Therefore, in [7], the direct proof of assignment of the lines 656.8 $\pm$0.2 cm^{-1} and 641.8 $\pm$1 cm^{-1} with localised vibration mode of σ-polaron lattice was obtained.

To explain differences in RS spectral characteristics by the change of the direction of the excitation wave propagation, we have to take into consideration the following. The possibility of spin wave resonance excitation in 1D-systems is strongly dependent on the geometry of experiment, determined by directions of chain axis, vectors of external static magnetic field (intracrystalline electric field) and oscillating magnetic (electric) fields by FMSWR (FESWR) study correspondingly. It is confirmed by FMSWR study in carbynes, [19]. The shape of CZSNTs is not strictly cylidric in the end of ion run and the axes x_i, $i = \overline{1,n}$ are generatrixes of the figure of onion-like shape, that provides the necessary geometry for AFESWR-excitation on σ-polaron lattice in opposite to ion beam direction. Moreover, the appearance of very broad line, Figure 2, seems to be indication on the excitation of the Fröhlich movement of σ-polaron lattice itself. The presence of Fröhlich sliding of σ-polaron lattice allows to explain qualitatively the appearance of "hysteresis" in spectral dependences relatively change of the direction of exciting laser wave propagation into opposite direction. It follows from energy law conservation position. Really, moving σ-polaron lattice possesses by kinetic energy. It means, that it is required lesser energy value to excite the local σ-polaron vibration mode in given case in correspondence with observation.

Therefore, CZSNTs incorporated in diamond matrix represent themselves the example of the system, which strongly interact with EM-field.

The appearance of the lines in IR spectra of another quasi 1D-system - heavily doped carbynes - in the range $(3500 - 5000)$ cm^{-1} with peak positions correspondingly at 3729.1 ± 4, 3956.2 ± 10 cm^{-1}, 4409.2 ± 4 cm^{-1}, 4720.8 ± 10 cm^{-1} in the spectrum of A-sample, Figure 3, and at 3892.6 ± 4 cm^{-1}, 4174.6 ± 4 cm^{-1}, 4420.3 ± 4 cm^{-1} in the spectrum of B-sample, Figure 4, seems to be direct indication of the emergence in given samples of longlived coherent state, determined by the space propagation of quantum Rabi oscillations. Really, in the work [24] was established theoretically, that in the case of strong electron-(spin)-photon interaction, there is the possibility to observe optical spectra in the same samples in usual deterministic regime and in stochastic regime by the change of registration conditions. It was concluded immediately from mathematical structure of new difference-differencial equations for dynamics of spectroscopic transitions for both radio- and optical spectroscopy (instead Bloch equations) for the model, representing itself the 1D-chain of N two-level equivalent elements coupled by exchange interaction (or its optical analogue for the optical transitions) between themselves and interacting with quantized EM-field and quantized lat-

tice deformation (phonon) field. The switch to stochastic regime has been achieved by observation of both ferroelectric spin wave resonance and antiferroelectric spin wave resonance [26], [24] by means of IR-reflection, absorption and transmittance spectroscopy in the same carbynoid samples. It seems to be undestandable, that coherence will get broken in stochastic regime resulting in disappearance in the spectra of the lines determined by the space propagation of quantum Rabi oscillations. At the same time, if the lines in spectral range $(3500-5000)$ cm^{-1} belong to the so called second order transitions, then they have to be presenting in stochastic regime too, especially if to take into account, that in deterministic regime they are registered with the amplitude of the same order with main lines, see Figure 3. We see from Figure 2 in [24], that actually the lines in spectral range $(3500-5000)$ cm^{-1} disappeared, instead lines the quantum noise is appeared with the average amplitude almost linearly increasing with frequency increase in the range $(3500-5000)$ cm^{-1}. In the favour of the interpretation proposed shows also the analysis of the shape of the line at 4409.2 ± 4 cm^{-1} in IR-spectrum of A-sample, Figure 3, and the line at 4420.3 ± 4 cm^{-1} in IR-spectrum of B-sample, Figure 4, which are not overlapped with other spectral lines.

It is seen, that given lines have characteristic asymmetric Dyson shape [33]. Dyson shape of spectral lines is characteristic, for instance, for ESR absorbtion in metals or in low-resistance semiconductors and it is determined by the space dispersion contribution [34], which is appeared in conductive media to be consequence of phase change of propagating EM-wave and/or spin polarization transfer itself. It was shown in [34], that, for example, in the case of static paramagnetic centers (that is without spin polarization transfer) in conductive media the space dispersion contribution and absorption contribution to resulting ESR responce is 1 to 1 (for the samples, thickness of which is greatly exceeds the scin-layer depth). It seems to be understandable, that the propagation of Rabi oscillations will lead qualitatively to the same picture, that is, to the space dispersion contribution in the IR-absorption, or IR-reflection response, that actually takes place, Figures 3, 4.

Therefore, experimental detection of Rabi wave packets confirms on the one hand the theory, elaborated in [5], [7] and reviewed in given Section. It was also the first experimental confirmation of Rabi wave phenomenon, predicted in [4], on the other hand. It means also, that semiclassical description of spectroscopic transitions in quasi-1D CZSNTs and in the systems like them cannot be appropriate. It substantially raises the practical concernment of QED-theory, especially, if to take into account, that the space propagation of quantum Rabi oscillation leads to formation of coherent states with very long life times, that has great significance for a number of practical applications, in particular, by elaboration of logic quantum systems including quantum computers and quantum communication systems.

The requirement of one-dimemensionality is substantial for applicability of Slater principle to CZSNTs [5], at the same time the Rabi wave phenomenon seems to be general and can be observed in 2D and 3D-systems. In given Section we reconsider the interpretation of Raman spectra in new 2D carbon material - graphene. Two kinds of modes are observed in Raman spectra of graphene, the so called first-order RS-peak G and so called second-order lines including $2D$-mode [35], which is attributed to D-peak overtone. G-mode is inerpreted to be zone-center optical modee [35]. So-called D- and G-bands lie in carbon materials at around (1330-1360) cm^{-1} and 1580 cm^{-1} respectively for visible excitation. The D-peak is usually very intense in amorphous carbon samples, while it is absent in perfect graphitic samples and in graphene. The D-peak according to [36] corresponds to modes associated with transverse optical phonons around the edge of the Brillouin zone. In the molecular picture, it is associated with the breathing mode of the sp^2 aromatic rings [37], [38]. It is also very remarkable, that $2D$-mode, which is observed in the range (2660 - 2710) cm^{-1} is always visible even when the D-peak is absent. Given peculiar behavior is interpreted in the literature by the double resonance activation mechanism of the D-peak [40], which requires the presence of defects for its initiation. The following explanation was proposed. In a double resonance process, Raman scattering is a four-step process: (i) a laser induced generation of an electron-hole pair; (ii) electron-phonon scattering with an exchanged momentum $\vec{q}\ \vec{K}$; (iii) electron scattering from a defect, whose recoil absorbs the momentum of the electron-hole pair; (iv) electron-hole recombination. The requirements of conservation of energy and momentum can only be satisfied by a defect presence. In a perfect sample, momentum conservation would be violated by the double resonance mechanism, and thus the D-peak is absent. Momentum conservation however is always satisfied in the case of the $2D$-peak, without the need for defect activation, since the process involves two phonons with opposite momentum vectors.

Given explanation of absence of D-peak in perfect graphitic samples and in graphene seems to be vague, especially if to take into consideration, that D-peak at 1332 cm^{-1} is marvelously observed in perfect diamond single crystals without additional requirement of structural defect presence. The range (2660 - 2710) cm^{-1} of observation of $2D$-peak indicates on rather large deviation from precisely twice frequency value. Therefore, it seems to be reasonable to assign D-peak with sp^3 bond hybridization, then its absence in perfect graphitic samples and in graphene becomes natural explanation. It means in its turn, that $2D$-peak has quite different origin.

It seems to be essential, that along with $2D$-peak the other lines were detected. So in [35], the first-order RS-peak G was detected in the vicinity of 1580 cm^{-1} and so called second-order lines were observed around 2480, 2700 ($2D$ band), 3250 cm^{-1} by $\lambda_{exc} = 488$ nm. It is

especially interesting, that the intensity of the second-order $2D$-band was found to be substantially exceeding the intensity of the corresponding first-order line G [35]. It was roughly four times the intensity of the G peak by $\lambda_{exc} = 488$ nm. At the same time $2D$-band was strongly suppressed and the lines at 2480, 3250 cm^{-1} were even not detected under ultraviolet (UV) excitation with λ_{exc} = 325 nm [35], that was not explained. Moreover, the $2D$-band under UV excitation shifts to the larger wave numbers and is found near 2825 cm^{-1}. At the same time the G-peak on all spectra appears at the same position at 1580 cm^{-1}. The shift of about 185 cm^{-1} of $2D$-peak from double D-peak frequency value seems to be too large to ascribe given line to D-peak overtone.

It is also seen, that theoretical dependence of $2D$-band position on excitation energy in the framework of the resonant Raman scattering model, presented in [35] by Figure 5, is far from experimental dependence. At the same time the suggestion, that "the second-order" lines are spectral mapping of revival part of Rabi wave packet, corresponding to the first-order line G, is agreeing with experimental data in [35] very well, see Figure 5 in our paper. The dependence, presented in Figure 5, was built from experimental data in [35] by choosing instead the energy the electrical component of oscillating excitation field to be x-coordinate. It is seen, that given experimental dependence is linear in full correspondence with expected for the center of Fourier transform of revival part of Rabi wave packets. It is analogue of aforesaid well known in radiospectroscopy linear dependence of Rabi oscillation frequency on magnetic component of oscillating excitation field, see, for instance, [17], [18].

Strong suppression of the "second order lines" including vanishing the lines at 2480, 3250 cm^{-1} under UV excitation with λ_{exc} = 325 nm can be easily explained by essentially more wide spectrum of nonresonance phonons, taking part in relaxation processes under UV excitation in comparison with the spectrum of nonresonance phonons under excitation with visible light. It is well known, that it leads to strong supression of quantum Rabi oscillation [39] and the peculiarity, consisting in strong suppression of the "second order lines" becomes therefore the natural explanation.

Thus, the experimental results presented [35] are in fact experimental evidence for the formation and propagation of Rabi wave packets in graphene. It seems to be evident, that Rabi wave packets can also be identified in free standing 2D-NTs by the production technology improvement.

Similar explanation can be proposed for transitions in heavily boron-doped diamond in the region of 1400-2800 cm^{-1} [41]. It means, that the theory of Rabi wave formation, presented in [4] for quasi-1D-systems can be developed and generalized for 2D- and 3D-systems.

III. FORMATION OF LONGLIVED COHERENT RESONANCE PHONON SYSTEM BY SPECTROSCOPIC TRANSITIONS

It has been established in recent work [8], that by strong dipole-photon and dipole-phonon coupling the formation of longlived coherent system of the resonance phonons takes place, and relaxation processes acquire pure quantum character. It is determined by the appearence of coherent emission process of EM-field energy, for which the resonance phonon system is responsible. Emission process is accompanying by phonon Rabi quantum oscillations, which can be time-shared from photon quantum Rabi oscillations, accompanying coherent absorption process of EM-field energy. For the case of radiospectroscopy it corresponds to the possibility of the simultaneous observation along with (para)magntic spin resonance the acoustic spin resonance.

Let us reproduce the proof of given conclusion for the convenience of readers in details.

Given work is development of the work [24], where the system of difference-differencial equations for dynamics of spectroscopic transitions for both radio- and optical spectroscopy for the model, representing itself the 1D-chain of N two-level equivalent elements coupled by exchange interaction (or its optical analogue for the optical transitions) between themselves and interacting with quantized EM-field and quantized phonon field its optical has recently been derived. Naturally the equations are true for any 3D system of paramagnetic centers (PC) or optical centers by the absence of exchange interaction. In given case the model presented differs from Tavis-Cummings model [3] by inclusion into consideration of quantized phonon system, describing the relaxation processes from quantum fied theory position. Seven equations for the seven operator variables, describing joint system {field + matter} can be presented in matrix form by three matrix equations. They are the following

$$\frac{\partial}{\partial t}\begin{bmatrix}\hat{\sigma}_l^- \\ \hat{\sigma}_l^+ \\ \hat{\sigma}_l^z\end{bmatrix} = 2\,\|g\|\begin{bmatrix}\hat{F}_l^- \\ \hat{F}_l^+ \\ \hat{F}_l^z\end{bmatrix} + ||\hat{R}_{\vec{q}l}^{(\lambda)}||, \tag{25}$$

$$\frac{\partial}{\partial t}\begin{bmatrix}\hat{a}_{\vec{k}} \\ \hat{a}_{\vec{k}}^+\end{bmatrix} = -i\omega_{\vec{k}}||\sigma_P^z||\begin{bmatrix}\hat{a}_{\vec{k}} \\ \hat{a}_{\vec{k}}^+\end{bmatrix} + \frac{i}{\hbar}\begin{bmatrix}-\sum\limits_{l=1}^{N}(\hat{\sigma}_l^+ + \hat{\sigma}_l^-)v_{l\vec{k}}^* \\ \sum\limits_{l=1}^{N}(\hat{\sigma}_l^+ + \hat{\sigma}_l^-)v_{l\vec{k}}\end{bmatrix}, \tag{26}$$

$$\frac{\partial}{\partial t}\begin{bmatrix}\hat{b}_{\vec{k}}\\ \\ \hat{b}^{+}_{\vec{q}}\end{bmatrix} = -i\omega_{\vec{q}}||\sigma^{z}_{P}||\begin{bmatrix}\hat{b}_{\vec{q}}\\ \\ \hat{b}^{+}_{\vec{q}}\end{bmatrix} + \frac{i}{\hbar}\begin{bmatrix}-\sum\limits_{l=1}^{N}\hat{\sigma}^{z}_{l}\lambda_{\vec{q}l}\\ \\ \sum\limits_{l=1}^{N}\hat{\sigma}^{z}_{l}\lambda_{\vec{q}l}\end{bmatrix} \quad (27)$$

where

$$\begin{bmatrix}\hat{\sigma}^{-}_{l}\\ \\ \hat{\sigma}^{+}_{l}\\ \\ \hat{\sigma}^{z}_{l}\end{bmatrix} = \hat{\vec{\sigma}}_{l} = \hat{\sigma}^{-}_{l}\vec{e}_{+} + \hat{\sigma}^{+}_{l}\vec{e}_{-} + \hat{\sigma}^{z}_{l}\vec{e}_{z} \quad (28)$$

is vector-operator of spectroscopic transitions for lth chain unit, $l = \overline{2, N-1}$ [24]. Its components, that is, the operators

$$\hat{\sigma}^{jm}_{v} \equiv |j_{v}\rangle\langle m_{v}| \quad (29)$$

are set up in correspondence to the states $|j_v\rangle$,$\langle m_v|$, where $v = \overline{1, N}$, $j = \alpha, \beta$, $m = \alpha, \beta$. For instance, the relationships for commutation rules are

$$[\hat{\sigma}^{lm}_{v}, \hat{\sigma}^{pq}_{v}] = \hat{\sigma}^{lq}_{v}\delta_{mp} - \hat{\sigma}^{pm}_{v}\delta_{ql}. \quad (30)$$

Further

$$\begin{bmatrix}\hat{F}^{-}_{l}\\ \\ \hat{F}^{+}_{l}\\ \\ \hat{F}^{z}_{l}\end{bmatrix} = \hat{\vec{F}} = \left[\hat{\vec{\sigma}}_{l} \otimes \hat{\vec{\mathcal{G}}}_{l-1,l+1}\right], \quad (31)$$

where vector operators $\hat{\vec{\mathcal{G}}}_{l-1,l+1}$, $l = \overline{2, N-1}$, are given by the expressions

$$\hat{\vec{\mathcal{G}}}_{l-1,l+1} = \hat{\mathcal{G}}^{-}_{l-1,l+1}\vec{e}_{+} + \hat{\mathcal{G}}^{+}_{l-1,l+1}\vec{e}_{-} + \hat{\mathcal{G}}^{z}_{l-1,l+1}\vec{e}_{z}, \quad (32)$$

in which

$$\hat{\mathcal{G}}^{-}_{l-1,l+1} = -\frac{1}{\hbar}\sum_{\vec{k}}\hat{f}_{l\vec{k}} - \frac{J}{\hbar}(\hat{\sigma}^{-}_{l+1} + \hat{\sigma}^{-}_{l-1}), \quad (33a)$$

$$\hat{\mathcal{G}}^{+}_{l-1,l+1} = -\frac{1}{\hbar}\sum_{\vec{k}}\hat{f}_{l\vec{k}} - \frac{J}{\hbar}(\hat{\sigma}^{+}_{l+1} + \hat{\sigma}^{+}_{l-1}), \quad (33b)$$

$$\hat{\mathcal{G}}^{z}_{l-1,l+1} = -\omega_{l} - \frac{J}{\hbar}(\hat{\sigma}^{z}_{l+1} + \hat{\sigma}^{z}_{l-1}). \quad (33c)$$

Here operator $\hat{f}_{l\vec{k}}$ is

$$\hat{f}_{l\vec{k}} = v_{l\vec{k}}\hat{a}_{\vec{k}} + \hat{a}^{+}_{\vec{k}}v^{*}{}_{l\vec{k}}. \quad (34)$$

In relations (33) J is the exchange interaction constant in the case of magnetic resonance transitions or its optical analogue in the case of optical transitions, the function $v_{l\vec{k}}$ in (34) is

$$v_{l\vec{k}} = -\frac{1}{\hbar}p^{jm}_{l}(\vec{e}_{\vec{k}} \cdot \vec{e}_{\vec{P}_{l}})\mathfrak{E}_{\vec{k}}e^{-i\omega_{\vec{k}}t + i\vec{k}\vec{r}}, \quad (35)$$

where p^{jm}_{l} is matrix element of operator of magnetic (electric) dipole moment $\vec{P}_{l}$ of l-th chain unit between the states $|j_l\rangle$ and $|m_l\rangle$ with $j \in \{\alpha, \beta\}$, $m \in \{\alpha, \beta\}$, $j \neq m$, $\vec{e}_{\vec{k}}$ is unit polarisation vector, $\vec{e}_{\vec{P}_{l}}$ is unit vector along $\vec{P}_{l}$-direction, $\mathfrak{sE}_{\vec{k}}$ is the quantity, which has the dimension of magnetic (electric) field strength, $\vec{k}$ is quantized EM-field wave vector, the components of which get a discrete set of values, $\omega_{\vec{k}}$ is the frequency, corresponding to $\vec{k}$th mode of EM-field, $\hat{a}^{+}_{\vec{k}}$ and $\hat{a}_{\vec{k}}$ are EM-field creation and annihilation operators correspondingly. In the suggestion, that the contribution of spontaneous emission is relatively small, we will have $p^{jm}_{l} = p^{mj}_{l} \equiv p_{l}$, where $j \in \{\alpha, \beta\}$, $m \in \{\alpha, \beta\}$, $j \neq m$. Further matrix $||\hat{R}^{(\lambda)}_{\vec{q}l}||$ is

$$||\hat{R}^{(\lambda)}_{\vec{q}l}|| = \frac{1}{i\hbar}\begin{bmatrix}2\hat{B}^{(\lambda)}_{\vec{q}l}\hat{\sigma}^{-}_{l}\\ \\ -2\hat{B}^{(\lambda)}_{\vec{q}l}\hat{\sigma}^{+}_{l}\\ \\ 0\end{bmatrix} \quad (36)$$

Here $\hat{B}^{(\lambda)}_{\vec{q}l}$ is

$$\hat{B}^{(\lambda)}_{\vec{q}l} = \sum_{\vec{q}}\lambda_{\vec{q}l}(\hat{b}^{+}_{\vec{q}} + \hat{b}_{\vec{q}}), \quad (37)$$

$\hat{b}^{+}_{\vec{q}}$ ($\hat{b}_{\vec{q}}$) is the creation (annihilation) operator of the phonon with impulse $\vec{q}$ and with energy $\hbar\omega_{\vec{q}}$, $\lambda_{\vec{q}l}$ is electron-phonon coupling constant. In equations (26) and (27) $\|\sigma^{z}_{P}\|$ is Pauli z-matrix, $\|g\|$ in equation (25) is diagonal matrix, numerical values of its elements are dependent on the basis choice. It is at appropriate basis

$$\|g\| = \begin{bmatrix}1 & 0 & 0\\ 0 & 1 & 0\\ 0 & 0 & 1\end{bmatrix}. \quad (38)$$

Right hand side expression in (31) is vector product of vector operators. It can be calculated by using of known expression (39) with additional coefficient $\frac{1}{2}$ the only, which is appeared, since

$$\left[\hat{\vec{\sigma}}_{l} \otimes \hat{\vec{\mathcal{G}}}_{l-1,l+1}\right] = \frac{1}{2}\begin{vmatrix}\vec{e}_{-} \times \vec{e}_{z} & \hat{\sigma}^{-}_{l} & \hat{\mathcal{G}}^{-}_{l-1,l+1}\\ \vec{e}_{z} \times \vec{e}_{+} & \hat{\sigma}^{+}_{l} & \hat{\mathcal{G}}^{+}_{l-1,l+1}\\ \vec{e}_{+} \times \vec{e}_{-} & \hat{\sigma}^{z}_{l} & \hat{\mathcal{G}}^{z}_{l-1,l+1}\end{vmatrix}', \quad (39)$$

the products of two components of two vector operators are replaced by anticommutators of corresponding components. Given detail is mapped by symbol $\otimes$ in (31) and by symbol $'$ in determinant (39). The equation, which is given by (25) is QED-generalization of semiclassical Landau-Lifshitz (L-L) equation for dynamics of spectroscopic transitions in a chain of exchange coupled centers derived in [25] and solved analytically in [24]. In comparison with semiclassical description, where the description of dynamics of spectroscopic transitions is exhausted by one vector L-L equation equation, in the case

of completely quantum consideration L-L type equation describes the only one subsystem of three-part-system, which consist of EM-field, dipole moments' (magnetic or electric) matter subsystem and phonon subsystem. It was concluded in [24], that the presence of additional equations for description of transition dynamics by QED model in comparison with semiclassical model leads to a number of new effects, which can be predicted the only by QED consideration of resonance transition phenomena. One of new effect was described in [24], starting the only from the mathematical structure of the equations. It was argued, that the equations (25), (26) represent themselves vector-operator difference-differential generalization of the system, which belongs to well known family of equation systems - Volterra model systems, widely used in biological tasks of population dynamics studies, which in its turn is generalization of Verhulst equation. In other words, it was predicted, for instance, that by some parameters in two-sybsystem Volterra model the stochastic component in solution will be appeared. Given prediction has aforesaid experimental confirmation by the study of optical properties in carbynes [26] indicating, that in given material strong electron-photon interaction is realized, which allows to explain the possibility to observe the stationary IR-reflection or absorption sspectra both in usual and in stochastic regime.

The terms like to right hand side terms in (27) were used in so called "spin-boson" Hamiltonian [42] and in so called "independent boson model" [43]. Given models were used to study phonon effects in a single quantum dot within a microcavity [44], [45], [46], [47], [39]. So, it has been shown in [47], [39], that the presence of the term in Hamiltonian [24]

$$\hat{\mathcal{H}}^{CPh} = \sum_{j=1}^{N} \sum_{\vec{q}} \lambda_{\vec{q}} (\hat{b}^{+}_{\vec{q}} + \hat{b}_{\vec{q}}) \hat{\sigma}^{z}_{j}, \tag{40}$$

which coincides with corresponding term in Hamiltonian in [47], [39] at $N = 1$ [contribution of given term to the equations for spectroscopic transitions is $\pm \sum_{l=1}^{N} \hat{\sigma}^{z}_{l} \lambda_{\vec{q}}$, see equation (27), (note that the equations for spectroscopic transitions were not derived in above cited works [44], [45], [46], [47], [39])] leads the only to exponential decrease of the magnitude of quantum Rabi oscillations with increase of electron-phonon coupling strength and even to their supression at relatively strong electron-phonon coupling.

However, by strong electron-photon coupling and strong electron-phonon coupling quite other picture of quantum relaxation processes becomes to be possible. Really, if to define the wave function of the chain system, interacting with quantized EM-field and with quantized lattice vibration field, to be vector of the state in Hilbert space over quaternion ring, that is quaternion function of quaternion argument, then like to [24] can be shown, that the equations (25) to (27) are Lorentz invariant and the transfer to observables can be realized. In particular, taking into account, that quaternion vector of the state is proportional to spin, the Hamiltonian, given by (40) describes in fact the interaction of phonon field with z-component S^z of the spin of matter subsystem. It seems to be reasonable to take into consideration the interaction of phonon field with S^+- and S^- components of the spin of matter subsystem. Therefore, in [8] in a natural way the following structure of Hamiltonian was proposed

$$\hat{\mathcal{H}} = \hat{\mathcal{H}}^{C} + \hat{\mathcal{H}}^{F} + \hat{\mathcal{H}}^{CF} + \hat{\mathcal{H}}^{Ph} + \hat{\mathcal{H}}^{CPh}, \tag{41}$$

where $\hat{\mathcal{H}}^{C}$ is chain Hamiltonian by the absence of the interaction with EM-field, $\hat{\mathcal{H}}^{F}$ is field Hamiltonian, $\hat{\mathcal{H}}^{CF}$ is Hamiltonian, describing the interaction between quantized EM-field and atomic chain. Hamiltonian $\hat{\mathcal{H}}^{C}$ is

$$\hat{\mathcal{H}}^{C} = \hat{\mathcal{H}}^{0} + \hat{\mathcal{H}}^{J}, \tag{42}$$

where $\hat{\mathcal{H}}^{0}$ is chain Hamiltonian in the absence of the interaction between structural elementary units of the chain. $\hat{\mathcal{H}}^{0}$ is given by the expression

$$\hat{\mathcal{H}}^{0} = \sum_{v=1}^{N} \sum_{m} E_{mv} |m_v\rangle\langle m_v|. \tag{43}$$

Here $m = \alpha, \beta$, E_{mv} are eigenvalues of $\hat{\mathcal{H}}^{0}$, which correspond to the states $|m_v\rangle$ of vth chain unit. Hamiltonian $\hat{\mathcal{H}}^{J}$ is

$$\hat{\mathcal{H}}^{J} = \sum_{n=1}^{N} [J_{E} (\hat{\sigma}^{+}_{n} \hat{\sigma}^{-}_{n+1} + \hat{\sigma}^{-}_{n} \hat{\sigma}^{+}_{n+1} + \frac{1}{2} \hat{\sigma}^{z}_{n} \hat{\sigma}^{z}_{n+1}) + H.c.]. \tag{44}$$

It is suggested in the model, that $|\alpha_n\rangle$ and $|\beta_n\rangle$ are eigenstates, producing the full set for each of N elements. It is evident, that given assumption can be realized strictly the only by the absence of the interaction between the elements. At the same time proposed model will rather well describe the real case, if the interaction energy of adjacent elements is much less of the energy of the splitting $\hbar\omega_0 = \mathcal{E}_{\beta} - \mathcal{E}_{\alpha}$ between the energy levels, corresponding to the states $|\alpha_n\rangle$ and $|\beta_n\rangle$. The case considered includes in fact all known experimental situations. Hamiltonian $\hat{\mathcal{H}}^{CF}$ of interaction of quantized EM-field with atomic chains was also represented in the set of variables, which includes the components of spectroscopic transition vector operator $\hat{\vec{\sigma}}_{v}$. It is in suggestion of dipole approximation and by fixed polarization of field components the following

$$\hat{\mathcal{H}}^{CF} = -\sum_{j=1}^{n} \sum_{l \neq m} \sum_{m} \sum_{\vec{k}} [p^{lm}_{j} \hat{\sigma}^{lm}_{j} (\vec{e}_{\vec{k}} \vec{e}_{\vec{P}_j}) \mathfrak{E}_{\vec{k}} \hat{a}_{\vec{k}} \times e^{-i\omega_{\vec{k}} t + i\vec{k}\vec{r}} + H.c.], \tag{45}$$

where p^{lm}_{j} is matrix element of operator of magnetic (electric) dipole moment $\vec{P}_j$ of j-th chain unit between the states $|l_j\rangle$ and $|m_j\rangle$ with $l_j = \alpha_j, \beta_j, m_j = \alpha_j, \beta_j$, $\vec{e}_{\vec{k}}$

is unit polarization vector, $\vec{e}_{\vec{P}_j}$ is unit vector along $\vec{P}_j$-direction, $\mathfrak{E}_{\vec{k}}$ is the quantity, which has the dimension of magnetic (electric) field strength, $\vec{k}$ is wave vector, $\hat{a}_{\vec{k}}$ is field annihilation operator. In the suggestion, that the contribution of spontaneous emission is relatively small, $p_j^{lm} = p_j^{ml} \equiv p_j$, where $l = \alpha, \beta, m = \alpha, \beta$. Then the function

$$q_{j\vec{k}} = -\frac{1}{\hbar} p_j (\vec{e}_{\vec{k}} \cdot \vec{e}_{\vec{P}_j}) \mathfrak{E}_{\vec{k}} e^{-i\omega_{\vec{k}} t + i\vec{k}\vec{r}} \tag{46}$$

was defined, and the expression (45) was rewritten in the form

$$\hat{\mathcal{H}}^{CF} = \sum_{v=1}^{n} \sum_{\vec{k}} [q_{j\vec{k}} (\hat{\sigma}_j^- + \hat{\sigma}_j^+) \hat{a}_{\vec{k}} + (\hat{\sigma}_j^- + \hat{\sigma}_j^+) \hat{a}_{\vec{k}}^+ q^*{}_{j\vec{k}}], \tag{47}$$

where $\hat{a}_{\vec{k}}^+$ is EM-field creation operator, $\hat{a}_{\vec{k}}$ is EM-field annihilation operator, superscript * in $q^*{}_{j\vec{k}}$ means complex conjugation. Field Hamiltonians have usual form

$$\hat{\mathcal{H}}^F = \sum_{\vec{k}} \hbar\omega_{\vec{k}} (\hat{a}_{\vec{k}}^+ \hat{a}_{\vec{k}} + \frac{1}{2}) \tag{48}$$

for EM-field and

$$\hat{\mathcal{H}}^{Ph} = \sum_{\vec{q}} \hbar\omega_{\vec{q}} (\hat{b}_{\vec{q}}^+ \hat{b}_{\vec{q}} + \frac{1}{2}) \tag{49}$$

for phonon field. Hamiltonian $\hat{\mathcal{H}}^{CPh}$ is

$$\hat{\mathcal{H}}^{CPh} = \hat{\mathcal{H}}_z^{CPh} + \hat{\mathcal{H}}_{\pm}^{CPh}, \tag{50}$$

where $\hat{\mathcal{H}}_z^{CPh}$ is determined by the expression

$$\hat{\mathcal{H}}_z^{CPh} = \sum_{j=1}^{N} \sum_{\vec{q}} (\lambda_{\vec{q}}^z \hat{b}_{\vec{q}} + (\lambda_{\vec{q}}^z)^* \hat{b}_{\vec{q}}^+) \hat{\sigma}_j^z. \tag{51}$$

Hamiltonian $\hat{\mathcal{H}}_{\pm}^{CPh}$ was represented in the following form

$$\hat{\mathcal{H}}_{\pm}^{CPh} = \sum_{j=1}^{N} \sum_{\vec{q}} \lambda_{\vec{q}}^{\pm} (\hat{\sigma}_j^- + \hat{\sigma}_j^+) \hat{b}_{\vec{q}} + (\lambda_{\vec{q}}^{\pm})^* (\hat{\sigma}_j^- + \hat{\sigma}_j^+) \hat{b}_{\vec{q}}^+. \tag{52}$$

Here $\lambda_{\vec{q}}^z$ and $\lambda_{\vec{q}}^{\pm}$ are electron-phonon coupling constants, which characterisire correspondingly the interaction with z- component S_j^z and with S^+- and S_j^- components of the spin of jth chain unit. It seems to be understandable, that they can be different in general case. Moreover, in order to take into account the interaction with both equilibrium and nonequilibrium phonons both the electron-phonon coupling constants have to be complex numbers, that takes proper account by expressions (51), (52). It has been shown, that ihe equations of the motion for spectroscopic transition operators $\hat{\vec{\sigma}}_l$, for quantized EM-field operators $\hat{a}_{\vec{k}}$, $\hat{a}_{\vec{k}}^+$ and for phonon field operators $\hat{b}_{\vec{q}}$, $\hat{b}_{\vec{q}}^+$ are the following. Instead equation (25) we have

$$\frac{\partial}{\partial t} \begin{bmatrix} \hat{\sigma}_l^- \\ \hat{\sigma}_l^+ \\ \hat{\sigma}_l^z \end{bmatrix} = 2 \|g\| \begin{bmatrix} \hat{F}_l^- \\ \hat{F}_l^+ \\ \hat{F}_l^z \end{bmatrix} + ||\hat{R}_{\vec{q}l}^{(\lambda^z)}|| + ||\hat{R}_{\vec{q}l}^{(\lambda^{\pm})}||, \tag{53}$$

where matrix $||\hat{R}_{\vec{q}l}^{(\lambda^z)}||$ is

$$||\hat{R}_{\vec{q}l}^{(\lambda^z)}|| = \frac{1}{i\hbar} \begin{bmatrix} 2\hat{B}_{\vec{q}l}^{(\lambda^z)} \hat{\sigma}_l^- \\ -2\hat{B}_{\vec{q}l}^{(\lambda^z)} \hat{\sigma}_l^+ \\ 0 \end{bmatrix} \tag{54}$$

with $\hat{B}_{\vec{q}l}^{(\lambda^z)}$, which is given by

$$\hat{B}_{\vec{q}l}^{(\lambda^z)} = \sum_{\vec{q}} [(\lambda_{\vec{q}l}^z)^* \hat{b}_{\vec{q}}^+ + \lambda_{\vec{q}l}^z \hat{b}_{\vec{q}}]. \tag{55}$$

Matrix $||\hat{R}_{\vec{q}l}^{(\lambda^{\pm})}||$ is

$$||\hat{R}_{\vec{q}l}^{(\lambda^z)}|| = \frac{1}{i\hbar} \begin{bmatrix} -\hat{B}_{\vec{q}l}^{(\lambda^{\pm})} \hat{\sigma}_l^z \\ \hat{B}_{\vec{q}l}^{(\lambda^{\pm})} \hat{\sigma}_l^z \\ \hat{B}_{\vec{q}l}^{(\lambda^{\pm})} (\hat{\sigma}_l^+ - \hat{\sigma}_l^-) \end{bmatrix}, \tag{56}$$

where $\hat{B}_{\vec{q}l}^{(\lambda^{\pm})}$ is

$$\hat{B}_{\vec{q}l}^{(\lambda^{\pm})} = \sum_{\vec{q}} [(\lambda_{\vec{q}l}^{\pm})^* \hat{b}_{\vec{q}}^+ + \lambda_{\vec{q}l}^{\pm} \hat{b}_{\vec{q}}]. \tag{57}$$

The equation (26) remains without changes. The equation (27) is

$$\frac{\partial}{\partial t} \begin{bmatrix} \hat{b}_{\vec{k}} \\ \hat{b}_{\vec{q}}^+ \end{bmatrix} = -i\omega_{\vec{q}} ||\sigma_P^z|| \begin{bmatrix} \hat{b}_{\vec{q}} \\ \hat{b}_{\vec{q}}^+ \end{bmatrix} + \frac{i}{\hbar} \begin{bmatrix} -\sum\limits_{l=1}^{N} \{\lambda_{\vec{q}l}^z \hat{\sigma}_l^z + \lambda_{\vec{q}l}^{\pm} (\hat{\sigma}_l^+ + \hat{\sigma}_l^-)\} \\ \sum\limits_{l=1}^{N} \{\lambda_{\vec{q}l}^z \hat{\sigma}_l^z + \lambda_{\vec{q}l}^{\pm} (\hat{\sigma}_l^+ + \hat{\sigma}_l^-)\} \end{bmatrix}. \tag{58}$$

Thus, QFT model for dynamics of spectroscopic transitions in 1D multiqubit exchange coupled system is generalized by taking into account the earlier proof [24], that spin vector is quaternion vector of the state of any quantum systen in Hilbert space defined over quaternion ring and consequently all the spin components has to be taken into account. New quantum phenomenon was predicted in [8]. The prediction results from the structure of the

equations derived and it consists in the following. The coherent system of the resonance phonons, that is, the phonons with the energy, equaled to resonance photon energy can be formed by resonance, that can lead to appearance along with Rabi oscillations determined by spin (electron)-photon coupling with the frequency Ω^{RF} of Rabi oscillations determined by spin (electron)-phonon coupling with the frequency Ω^{RPh}. In other words, QFT model predicts the oscillation character of quantum relaxation, that is quite different character in comparison with phenomenological and semiclassical Bloch models. Moreover, if $\mid \lambda_{\vec{q}l}^{\pm} \mid < g$ the second Rabi oscillation process will be observed by stationary state of two subsystems {EM-fied + magnetic (electric) dipoles}, that is, it will be registered in quadrature with the first Rabi oscillation process. It can be experimentally detected even by stationary spectroscopy methods.

IV. CONCLUSIONS

Brief review of the theoretical and experimental results, based mainly on the works of authors, in the application of quantum field theory to the study of carbon low-dimensional systems - quasi-1D carbon nanotubes, carbynes and graphene with emphasis on formation of longlived coherent states of joint photon-electron and joint resonance phonon-electron systems of given materials is presented. Two new ways for longlived coherent state formation are considered in present work, leading to essentially more long lifetimes in comparison with known methods of formation of individual coherent states, realised on point centers in crystals. The first way is the longlived coherent state formation in result of Rabi-wave packets' propagation in the materials with strong electron-photon interaction. Given mechanism was confirmed experimentally on examples of a number carbon low-dimensional materials - quasi-1D carbon nanotubes, carbynes, graphene. Naturally, the range of suitable materials for given aim is much wider.

Main difference of given states in comparison with individual coherent states, realised on point centers, that they are collective coherent states.

On the other hand the appearance of additional lines, associated with the same RS-mode, means, that strong electron-photon coupling takes place in quasi-1D CZSNTs, carbynes and graphene by interaction with EM-field and quantum nature of EM-field has to be taken into account in any experiments and practical application of quasi-1D CZSNTs carbynes and graphene with participation of EM-field. By strong electron-photon coupling all optical spectra, in particular, Raman spectra seem to be registered (in spite of the usage of stationary measurement technique) in nonequilibrium coherent state, which is the consequence of Rabi wave packets' formation and propagation.

QFT model for dynamics of spectroscopic transitions in 1D multiqubit exchange coupled system is generalized by taking into account the earlier proof [24], that spin vector is quaternion vector of the state of any quantum systen in Hilbert space defined over quaternion ring and consequently all the spin components has to be taken into account. New quantum phenomenon is predicted. The prediction results from the structure of the equations derived and it consists in the following. The coherent system of the resonance phonons, that is, the phonons with the energy, equaled to resonance photon energy can be formed by resonance, that can lead to appearance along with Rabi oscillations determined by spin (electron)-photon coupling with the frequency Ω^{RF} of Rabi oscillations determined by spin (electron)-phonon coupling with the frequency Ω^{RPh}. In other words QFT model predicts the oscillation character of quantum relaxation, that is quite different character in comparison with phenomenological and semiclassical Bloch models. Moreover if absolute value of electron-phonon coupling constant $|\lambda_{\vec{q}l}^{\pm}|$, which characterises the interaction with S^{+}- and S_j^{-} components of the spin of jth chain unit is less, than electron(spin)-photon coupling constant g, the model predicts, that the second quantum Rabi oscillation process will be observed by stationary state of joint two subsystems {EM-field + magnetic (electric) dipoles}, and it will be registered in quadrature with the first quantum Rabi oscillation process. The second quantum Rabi oscillation process is governed by the formation of the coherent system of the resonance phonons. Therefore along with absorption process of EM-field energy the coherent emission process takes place. Both the quantum Rabi oscillation processes can be time-shared. For the case of radiospectroscopy it corresponds to the possibility of the simultaneous observation along with (para)magnetic spin resonance the acoustic spin resonance. The second (acoustic) quantum Rabi oscillation process can be detected even by stationary spectroscopy methods.

New quantum phenomenon predicted opens the second way of the formation of the coherent states of joint system {magnetic (electric) dipoles + resonance phonons} in the matter. Both the phenomena of the formation of the coherent states in the matter can find a number of practical applications, in particular they can be used by elaboration of various logic quantum systems including quantum computers and quantum communication systems, in which quantized EM-field and/or quantized acoustic field will be working components. The same conclusion is concerned the elaboration of various optoelectronic and spintronic devices.

[1] Wang, D.-W.; Millis, A J and Das Sarma, S. *Solid State Commun.* **2004**, *131*, 637-645

[2] Jaynes E T and Cummings F W, Proc.IEEE **51**, (1963)

89
[3] Tavis M, Cummings F W, Phys.Rev., **170**(2) (1968) 387
[4] Slepyan G.Ya, Yerchak Y.D, Hoffmann A, Bass F.G, Phys.Rev.B, **81** (2010) 085115-085132
[5] Dovlatova A, Yearchuck D, Chem.Phys.Lett., **511** (2011) 151-155
[6] Dovlatova A, Yearchuck D, arXiv:1102.2619v2 [math-ph] 24 Feb 2011
[7] Yerchuck D, Dovlatova A, J.Phys.Chem.,C, DOI: 10.1021/jp205549b
[8] Dovlatova A, Yearchuck D,in press
[9] Su, W-P; Schrieffer, J.R; Heeger, A.J *Phys.Rev.Lett.* **1979**, *42*, 1698-1701
[10] Su, W-P; Schrieffer, J.R; Heeger, A.J *Phys.Rev.B* **1980**, *22*, 2099-2111
[11] Saito, R; Fujita, M; Dresselhaus, G; Dresselhaus, M.S *Appl.Phys.Lett.* **1992**, *60*, 2204-2206
[12] Saito, R; Fujita, M; Dresselhaus, G; Dresselhaus, M.S *Phys.Rev.B* **1992**, *46*, 1804-1811
[13] Farhat, H; Son, H; Samsonidze, G.G; Reich, S; Dresselhaus, M.S; Kong, J *Phys.Rev.Lett.* **2007**, *99*, 145506-1-4
[14] Farhat, H; Sasaki, K; Kalbac, M; Hofmann, M; Saito, R; Dresselhaus, M.S; Kong, J *Phys.Rev.Lett.* **2009**, *102*, 126804-1-4
[15] Jorio, A; Pimenta, M A; Filho, A.G.S; Saito, R; Dresselhaus, G; Dresselhaus, M.S *New J.Phys.* **2003**, *5*, 139-145
[16] Abragam A.I, The Principles of Nuclear Magnetism, Oxford Univ.Press, London, 1961, Nuclear Magnetism, Iz.In.Lit., M., 1963, 551 pp
[17] Yerchak, D.P; Rutkovskii, I.Z; Stelmakh, V.F; Fedoruk, G G, in "Radiation Damage Physics and Radiation Materialkeeping", Kharkov, 1982, 2/21, 79-80
[18] Fedoruk, G G; Rutkovskii, I.Z;, Yerchak, D.P; Stelmakh, V.F, *Sov.J.Exp.Theor.Physics*, USA **1981**, *80*, 2004-2009
[19] Ertchak D P, Kudryavtsev Yu P, Guseva M B, Alexandrov A F et al, J.Physics: Condensed Matter, **11**, N3 (1999) 855-870
[20] Heeger A.J, Kivelson S, Schrieffer J.R, Su W-P, Rev.Mod.Phys., **60** (1988) 781-850
[21] Erchak D.P, Efimov V.G, Zaitsev A M, Stelmakh V.F, Penina N.M, Varichenko VS, Tolstykh VP, Nucl.Instr.Meth in Phys.Res.B, **69** (1992) 443-451
[22] Ertchak D.P, Efimov V.G, Stelmakh V.F, J.Appl.Spectroscopy, **64**, N 4 (1997) 433-460
[23] Ertchak D.P, Efimov V.G, Stelmakh V.F, Martinovich V A, Alexandrov A F, Guseva M B, Penina N M, Karpovich I A, Varichenko V S, Zaitsev A M, Fahrner W R, Fink D, Physica Status Solidi, b, **203** N2, (1997) 529-548
[24] Yearchuck D, Yerchak Y, Dovlatova A, Optics Communications, **283** (2010) 3448-3458
[25] Yearchuck D, Yerchak Y, Red'kov V, Doklady NANB, **51**, N 5 (2007) 57-64
[26] Yearchuck D, Yerchak Y, Alexandrov A, Phys.Lett.A, **373**, N 4 (2009) 489-495
[27] Yearchuck, D; Yerchak, E, arXiv: 0709.3382 (2007)
[28] Yearchuck, D; Yerchak, Y; Kirilenko, A; Popechits, V *Doklady NANB* **2008**, *52*, 48-53
[29] Ertchak D.P, In "Carbyne and Carbynoid Structures", Series: Physics and Chemistry of Materials with Low Dimensional Structures, pp 357-369, Kluwer Academic Publishers, Dordrecht, Boston, London, Edited by Heimann R.B, Evsyukov S.E, Kavan L, 1999, 446 pp
[30] Kudryavtsev Yu.P, Yearchuck D.P, The European Material Conference. International Conference on Electronic Materials and European Materials Research Society Spring Meeting. E-MRS-IUMRS-ICEM 2000, Symposium E, Current Trends in Nanotechnologies, Strasbourg, France, May 30-June 2, 2000, E-I/P14, Book of Abstracts, E-11
[31] Yearchuck, D; Guseva, M; Alexandrov, A and v.Bardeleben, H-J, E-MRS 2004 Spring Meeting, Symposium I, Advanced Multifunctional Nanocarbon Materials and Nanosystems, Strasbourg, France, May 24-28, 2004, I/PI.09
[32] Yearchuck, D; Guseva, M; Alexandrov, A, 7th International Conference on Nanostructured Materials, NANO 2004, June 20-24, 2004, Wiesbaden, Germany, Extended Abstracts, 2.A32
[33] Dyson, F D *Phys.Rev.* **1955**, *98*, 349-359
[34] Erchak, D.P; Zaitsev, A M; Stel'makh, V.F; Tkachev, V D *Sov.Phys.Semicond.*, USA **1980**, *14*, 79-82
[35] Calizo, I; Bejenari, I; Rahman, M; Guanxiong Liu and Balandin, A *J.Appl.Phys.* **2009**, *106*, 043509–043512
[36] Ferrari, A *Sol.St.Comm.* **2007** 143, 47-57
[37] Tuinstra, F and Koenig, J *J.Chem.Phys.* **1970** 53, 1126-1130
[38] Ferrari, A and Robertson, J *Phys.Rev.B* **2000** 61, 14095-14107
[39] Ka-Di Zhu; Zhuo-Jie Wu; Xiao-Zhong Yuan and Hang Zheng *Phys.Rev.B* **2005**, *71*, 235312-235312-5
[40] Thomsen, C and Reich, S *Phys.Rev.Lett.* **2000**, *85*, 5214-5217
[41] Vlasov, I I; Ekimov, E A; Basov, A A; Goovaerts, E; Zoteev, A V arXiv:0801.1611v1 [cond-mat.mtrl-sci] (2008)
[42] Leggett A J, Chakravarty S Chakravarty, Dorsey A T, Fisher M P A, Garg A, Zwerger W, Rev.Mod.Phys., **59** (1987) 1-85
[43] Mahan G D, Many-Particle Physics, Plenum, New York, 2000
[44] Heitz R, Mukhametzhanov I, Stier O, Madhukar A, and Bimberg D, Phys.Rev.Lett.,**83** 1999 4654-4657
[45] Türck V, Rodt S, Stier O, Heitz R, Engelhardt R, Pohl U W, and Bimberg D, Phys.Rev.B, **61**, (2000) 9944-9947
[46] Besombes L, Kheng K, Marsal L, and Mariette H, Phys.Rev.B, **63** (2001) 155307-155307-5
[47] Wilson-Rae I and Imamoglu A, Phys.Rev.B, **65** (2002) 235311-235311-5

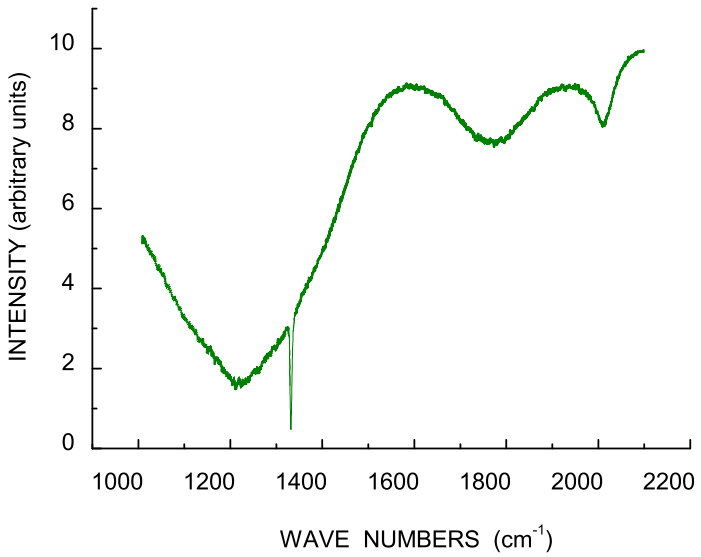
INTENSITY (arbitrary units)
0
2
4
6
8
10
1000
1200
1400
1600
1800
2000
2200
WAVE NUMBERS (cm-1)